

Original

## Distribution and Sequence of Pyknotic Cells in Rat Fetuses Exposed to Busulfan

Toko Ohira<sup>1</sup>, Ryo Ando<sup>2</sup>, Rie Andoh<sup>2</sup>, Tomomi Nakazawa<sup>2</sup>, Kaori Nishihara<sup>2</sup>, Satoshi Yamamoto<sup>3</sup>, Norihiko Nakamura<sup>3</sup>, and Kazutoshi Tamura<sup>2</sup>

<sup>1</sup>Hamamatsu Branch of Pathology Division, BOZO Research Center Inc., 164–2 Wada-cho, Higashi-ku, Hamamatsu, Shizuoka 435-0016, Japan

<sup>2</sup>Pathology Division, Gotemba Laboratories, BOZO Research Center Inc., 1284 Kamado, Gotemba, Shizuoka 412-0039, Japan

<sup>3</sup>Toxicology Division, Gotemba Laboratories, BOZO Research Center Inc., 1284 Kamado, Gotemba, Shizuoka 412-0039, Japan

**Abstract:** Busulfan, an antineoplastic bifunctional-alkylating agent, is known to induce developmental anomalies. In the present study, we examined the distribution and sequence of pyknotic cells in rat fetal tissues exposed to busulfan. Pregnant rats on gestation day 13 were administered intraperitoneally 30 mg/kg of busulfan, and fetal tissues were examined at 6, 12, 24, 36, 48, 72 and 96 hours after treatment (HAT). Pyknosis of component cells was observed markedly in the brain, moderately in the eyes and spinal cord and mildly in the craniofacial tissue, mandible, limb buds, tail bud, ganglions, alimentary tract, lungs, kidneys, pancreas and liver. In the brain, mitotic inhibition was also detected. Most of the pyknotic cells were considered to be apoptotic cells judging from the results of TUNEL staining and electron microscopic examination. Commonly in the above-mentioned tissues, pyknotic cells began to increase at 24 HAT, peaked at 36 or 48 HAT and disappeared at 96 HAT, which is when the histological picture returned to normal in most tissues except for the brain, spinal cord and eyes. The present study clarified the outline of busulfan-induced apoptosis in rat fetuses. (J Toxicol Pathol 2009; 22: 167–171)

**Key words:** busulfan, histopathology, pyknosis, fetal tissues, rat

### Introduction

Busulfan is a bifunctional alkylating agent used for treatment of chronic myeloid leukemia. However, busulfan is also known to have teratogenic and cytotoxic potential<sup>1</sup>, and it has been reported that busulfan induces microencephaly, microphthalmia, microtia, microrostellum, micrognathia, microabdomen, and brachydactylia in a number of animal species<sup>2–5</sup>. Recently, Furukawa *et al.*<sup>3</sup> examined in detail the brain and eyes of rat fetuses obtained from dams administered 10 mg/kg/day of busulfan from gestation day (GD) 12 to 14 and demonstrated that busulfan induces apoptosis and mitotic inhibition in neuroepithelial cells of the fetal brain and eyes. They suggested that such extensive apoptosis and mitotic inhibition might be related to the induction of malformations in the brain and eyes.

Busulfan is easily absorbed; distributes to the spleen, bone marrow, liver, kidneys and lungs; and rapidly disappears from blood circulation in adults<sup>6–9</sup>. In addition, it has been reported that the main target of the cytotoxic effects of busulfan is slowly proliferating or non-proliferating stem cell compartments in such tissues as the lungs<sup>10</sup>, gastrointestinal tissues<sup>11</sup>, lymphoid tissues<sup>12,13</sup>, gonadal tissues<sup>4</sup> and neural tissues<sup>11</sup> in humans and animals. However, there are no available data on such stem cell compartments in fetal tissues, and the whole area of busulfan-induced fetotoxicity has not yet been fully elucidated.

In the present study, as a first step to clarify the histopathological nature of busulfan-induced fetotoxicity, histopathological examinations were carried out on fetal tissues obtained from dams exposed to busulfan on GD 13, focusing on the distribution and sequence of pyknotic cells. In addition, we attempted to compare busulfan-induced central nervous system (CNS) lesions with other DNA-damaging agents-induced lesions. In this connection, GD 13 has been reported to be the most sensitive period of the rat fetal CNS to DNA-damaging agents<sup>14–19</sup>.

---

Received: 1 January 2009, Accepted: 22 April 2009

Mailing address: Toko Ohira, Branch of Pathology Division, BOZO Research Center Inc., 164-2 Wada-cho, Higashi-ku, Hamamatsu, Shizuoka 435-0016, Japan  
TEL&FAX: 81-53-467-1002  
E-mail: ohira-toko@bozo.co.jp

## Materials and Methods

### Animals

Forty-two pregnant Crl:CD (SD) rats on GD 10 were obtained from Charles River Japan Inc. (Kanagawa, Japan). The animals were housed individually in plastic cages in an environmentally controlled room (temperature:  $23 \pm 3^\circ\text{C}$ ; relative humidity:  $55 \pm 20\%$ ; ventilation rate: 10–15 times per hour; and 12h/12h light /dark cycle) and fed a commercial diet (CRF-1; Oriental Yeast Co., Ltd., Tokyo, Japan) and tap water *ad libitum*. The protocol of this study was reviewed and approved by the Animal Care and Use Committee of Bozo Research Center.

### Chemical and dosage

Busulfan (Sigma, St. Louis, MO, USA) was suspended with olive oil. The dose (30 mg/kg) of busulfan used in the present study was determined based on the results of a preliminary study, in which dams were administered intraperitoneally busulfan at a single dose of 10, 30 or 50 mg/kg on GD 13.

### Experimental designs

Forty-two animals were equally divided into the control and busulfan groups. The animals of the busulfan group were administered intraperitoneally 30 mg/kg of busulfan, and those of the control group were administered intraperitoneally 10 mL/kg of olive oil on GD 13. Three dams of each group were sacrificed by exsanguination from the abdominal aorta under diethyl ether anesthesia at 6, 12, 24, 36, 48, 72 and 96 hours after busulfan-treatment (HAT), respectively. At necropsy, the body weights of dams and fetuses and litter sizes were recorded.

### Histopathology

All fetuses were weighed and fixed with 10% phosphate-buffered formalin (pH 7.2). A total of 10 fetuses each of the control and busulfan groups were obtained randomly from dams at each time-point (3 or 4 fetuses/dam). Four- $\mu\text{m}$  paraffin sections were stained with hematoxylin and eosin (HE) and subjected to histopathological examinations.

### In situ detection of fragmented DNA

DNA fragmentation was examined by the terminal deoxynucleotidyl transferase-mediated dUTP end labeling (TUNEL) method, which was first proposed by Gavrieli *et al.*<sup>20</sup> and has been widely used for the detection of apoptotic cells, using a commercial apoptosis detection kit (Chemicon Inc., Gaithersburg, MD, USA). In brief, multiple fragmentation DNA<sup>3'-OH</sup> ends on the section were labeled with digoxigenin-dUTP in the presence of terminal deoxynucleotidyl transferase (TdT). Peroxidase-conjugated anti-digoxigenin antibody was then reacted with the sections. Apoptotic nuclei were visualized by peroxidase-diaminobenzidine (DAB) reaction. The sections were then counterstained with methyl green.

### Electron microscopy

Small pieces of the telencephalic wall (2 fetuses each from 2 dams of the control and busulfan groups) were obtained at 48 HAT. They were fixed in 0.5% glutaraldehyde/1.5% paraformaldehyde in 0.1 M phosphate buffer (pH 7.4), postfixed in 1% osmium tetroxide in the same buffer and embedded in epoxy resin (Nissin EM Co., Ltd., Tokyo, Japan). Ultrathin sections of the selected blocks were double-stained with uranyl acetate and lead citrate and observed under a JEM-100CXII electron microscope (JEOL Ltd., Tokyo, Japan).

### Statistical analysis

Numerical data were expressed as the Mean  $\pm$  standard deviation (SD). For the numerical data, the homogeneity of variance in the control and busulfan groups were analyzed by the F test (level of significance: 5%, two-tailed), and the homogeneous data were analyzed by the Student's *t*-test (level of significance: 1%, two-tailed), while the heterogeneous data were analyzed by the Aspin-Welch *t*-test (level of significance: 1%, two-tailed) for the group mean difference between the control and busulfan groups.

## Results

### Mortality, bodyweights of dams and fetuses and litter size

No deaths occurred in any dams of the control and busulfan groups. The body weights of the dams in the busulfan group were reduced from 24 to 96 HAT compared with those in the control group, but there were no significant differences between the two groups (Fig. 1). There were no

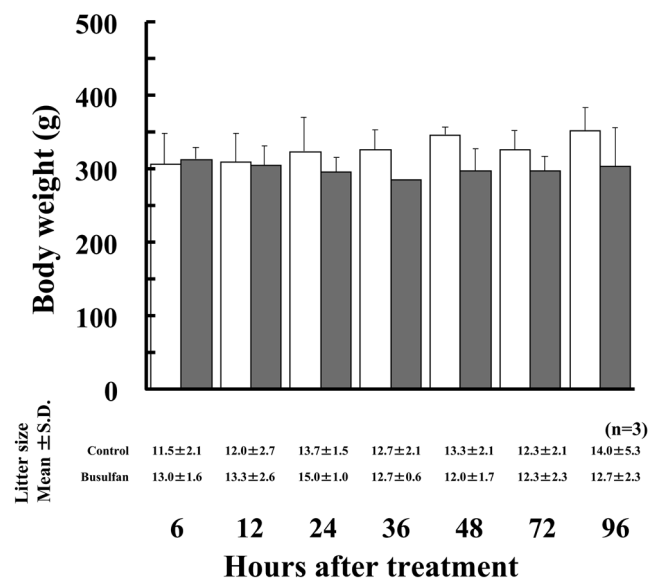
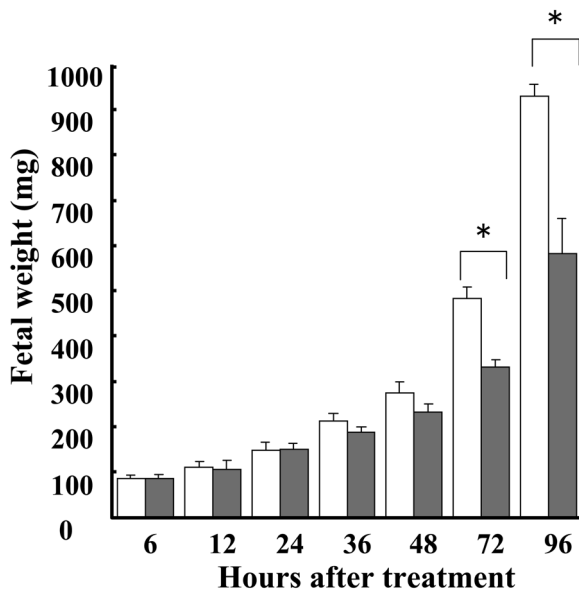


Fig. 1. Changes in the body weights of dams and litter size. □: Control group. ■: Busulfan group. n: Number of dams. Body weight is shown as the mean  $\pm$  SD.



**Fig. 2.** Changes in fetal weights. □: Control group. ■: Busulfan group. Fetal weight is shown as the mean  $\pm$  SD. \* $p < 0.01$ : Significantly different from the control group.

differences in litter size between the control and busulfan groups (Fig 1). The fetal body weights of the busulfan group were significantly reduced at 72 and 96 HAT compared with those of the control group (Fig. 2).

### Histopathological changes

In the busulfan group, pyknotic cells were observed markedly in the brain (telencephalon, diencephalon, mesencephalon and metencephalon), moderately in the eyes (retina and lens) and spinal cord (dorsal layer) and mildly in the mesenchymal cells of the craniofacial tissues, mandible, limb buds and tail bud, dorsal root ganglions, epithelial cells of the alimentary tract, lungs, kidneys and pancreas, and hepatocytes and hematopoietic progenitor cells were observed in the liver (Table 1 and Figs.3 and 4). The sequence of pyknotic cells was similar among the tissues affected, and the pyknotic cells began to increase at 24 HAT, peaked at 36 or 48 HAT and disappeared at 96 HAT (Table 1). For example, in the telencephalic wall (Fig. 5), a few pyknotic cells appeared mainly in the medial layer of the ventricular zone (VZ) at 24 HAT. At 36 HAT, pyknotic cells drastically increased in number in all layers of the VZ except for one or two cell layers facing the ventricle and in the cortical plate (CP). At 48 HAT, the density of neuroepithelial cells was reduced due to disappearance of dead cells, leaving irregular empty space in the VZ. From 36 to 48 HAT, the number of mitotic cells in the ventricular layer of the VZ was reduced in the busulfan group compared with the control group. At 72 HAT, pyknotic cells decreased, but still remained in the medial and dorsal layers of the VZ. At 96 HAT, pyknotic cells were no longer observed.

At 96 HAT, the histological picture returned to normal in most tissues except for the brain, spinal cord and eyes. In particular, the width of the VZ of the brain and dorsal layer of the spinal cord and the retinal thickness and lenticular size

**Table 1.** Distribution and Sequence of Pyknotic Cells in Rat Fetal Tissues Exposed to Busulfan

| Hours after treatment            | Control 0 mg/kg |    |    |    |    |    | Busulfan 30 mg/kg |   |    |    |     |     |    |    |
|----------------------------------|-----------------|----|----|----|----|----|-------------------|---|----|----|-----|-----|----|----|
|                                  | 6               | 12 | 24 | 36 | 48 | 72 | 96                | 6 | 12 | 24 | 36  | 48  | 72 | 96 |
| Central nervous system           |                 |    |    |    |    |    |                   |   |    |    |     |     |    |    |
| Telencephalon                    | -               | -  | -  | -  | -  | -  | -                 | - | -  | +  | +++ | +++ | ++ | -  |
| Diencephalon                     | -               | -  | -  | -  | -  | -  | -                 | - | -  | +  | +   | ++  | +  | -  |
| Mesencephalon                    | -               | -  | -  | -  | -  | -  | -                 | - | -  | +  | +   | ++  | +  | -  |
| Metencephalon                    | -               | -  | -  | -  | -  | -  | -                 | - | -  | +  | ++  | ++  | ±  | -  |
| Spinal cord                      | -               | -  | -  | -  | -  | -  | -                 | - | -  | +  | ++  | ++  | ±  | -  |
| Mesenchymal tissues              |                 |    |    |    |    |    |                   |   |    |    |     |     |    |    |
| Craniofacial                     | -               | -  | -  | -  | -  | -  | -                 | - | -  | +  | +   | +   | ±  | -  |
| Mandible                         | -               | -  | -  | -  | -  | -  | -                 | - | -  | ±  | +   | +   | ±  | -  |
| Limb buds                        | -               | -  | -  | -  | -  | -  | -                 | - | -  | +  | +   | +   | ±  | -  |
| Tail bud                         | -               | -  | -  | -  | -  | -  | -                 | - | -  | ±  | +   | +   | ±  | -  |
| Spinal ganglion                  | -               | -  | -  | -  | -  | -  | -                 | - | -  | ±  | +   | ±   | ±  | -  |
| Alimentary tract                 | -               | -  | -  | -  | -  | -  | -                 | - | -  | ±  | +   | +   | ±  | -  |
| Heart                            | -               | -  | -  | -  | -  | -  | -                 | - | -  | -  | -   | -   | -  | -  |
| Lungs                            | -               | -  | -  | -  | -  | -  | -                 | - | -  | ±  | +   | +   | ±  | -  |
| Kidneys                          | -               | -  | -  | -  | -  | -  | -                 | - | -  | ±  | ±   | ±   | ±  | -  |
| Pancreas                         | -               | -  | -  | -  | -  | -  | -                 | - | -  | ±  | ±   | ±   | -  | -  |
| Liver                            | -               | -  | -  | -  | -  | -  | -                 | - | -  | ±  | +   | +   | -  | -  |
| Hematopoietic cells in the liver | -               | -  | -  | -  | -  | -  | -                 | - | -  | ±  | +   | +   | ±  | -  |
| Eyes                             |                 |    |    |    |    |    |                   |   |    |    |     |     |    |    |
| Retina                           | -               | -  | -  | -  | -  | -  | -                 | - | -  | +  | ++  | ++  | +  | -  |
| Lens                             | -               | -  | -  | -  | -  | -  | -                 | - | -  | -  | +   | +   | ±  | -  |

Codes: -, ±, +, ++ and +++ indicate almost absent, minimal, mild, moderate and marked, respectively.

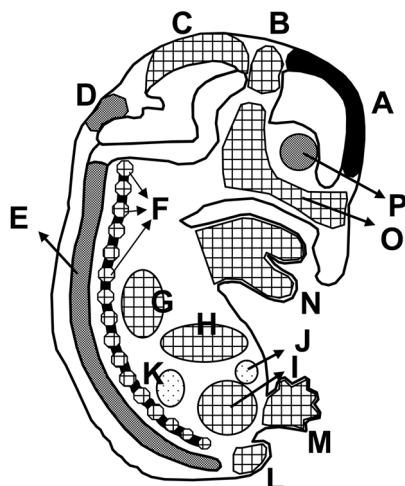


**Fig. 3.** Distribution and severity of pyknotic cells at 36 HAT in the fetal tissues. A: Telencephalon. B: Diencephalon. C: Mesencephalon. D: Metencephalon. E: Spinal cord. F: Ganglions. G: Lungs. H: Liver. I: Alimentary tract. J: Pancreas. K: Kidneys. L: Tail bud. M: Limb buds. N: Mandible. O: Craniofacial tissue. P: Eye. [···]: Minimal. [—]: Mild. [▨]: Moderate. [■]: Marked.

of the eyes were reduced in comparison with those of the controls.

The nuclei of almost all of the pyknotic cells were positively stained by the TUNEL method (Fig. 6). Moreover, in the electron microscopic examination, pyknotic cells showed shrinkage of the cell body with nuclear chromatin condensation, and some of the cells were fragmented into so-called apoptotic bodies, which were frequently ingested by adjacent cells and macrophages (Fig. 7).

## Discussion

In the present study, the distribution and sequence of pyknotic cells were examined in fetal tissues obtained from dams intraperitoneally treated with 30 mg/kg of busulfan on GD 13.

No deaths occurred in any dams and fetuses, and there was no difference in litter size between the control and busulfan groups. However, compared with those of the control group, the fetal weights of the busulfan group were significantly reduced at 72 and 96 HAT.

The histopathological changes in the brain and eyes roughly corresponded to those reported by Furukawa *et al.*<sup>3</sup> Moreover, in the present study, pyknosis was also detected in the component cells of the spinal cord, craniofacial tissue, mandible, limb buds, tail bud, ganglion, alimentary tract, lungs, kidneys, pancreas and liver. Apart from their severity, the sequence of pyknotic cells was similar among the above-mentioned tissues. Namely, pyknotic cells generally began to increase at 24 HAT, peak at 36 or 48 HAT and disappeared at 96 HAT, when the histological picture returned to normal in most tissues except for the brain, spinal

cord and eyes, in which histopathological changes such as reduction in size and cell density remained. In the brain, which was most severely damaged, a decrease in the number of mitotic cells located in the ventricular layer of the VZ was also detected. This suggests that apoptosis and growth inhibition of neuroepithelial cells occurred simultaneously in the busulfan group as previous reported in rat and mouse fetal brains exposed to other DNA damaging agents<sup>14–19, 21</sup>. The difference in the severity of pyknosis of component cells among the fetal tissues in the present study is considered to reflect the difference in the stage of their development on the day of busulfan exposure.

The nuclei of almost all of the above-mentioned pyknotic cells were positively stained by the TUNEL method. Moreover, these pyknotic cells showed electron microscopic characteristics of apoptotic cells. Therefore, it is reasonable to consider that these pyknotic cells were apoptotic. Thus, excessive apoptotic cell death induced in the above-mentioned fetal tissues by busulfan may result in induction of malformation in the corresponding tissues of neonates as mentioned previously.

The induction of apoptotic cell death in the CNS has also been reported for DNA-damaging agents such as 5-azacytidine<sup>16,22</sup>, ethylnitrosourea<sup>14</sup>, 1- $\beta$ -D-arabinofuranosylcytosine<sup>15</sup>, indole-3-acetic acid<sup>23</sup>, etoposide<sup>17</sup>, 5-fluorouracil<sup>18</sup>, 6-mercaptopurine<sup>21</sup> and hydroxyurea<sup>19</sup>, suggesting that the fetal CNS might be highly sensitive to genotoxic agents. The histopathological findings in the fetal CNS were essentially similar between the present data on busulfan and those on the above-mentioned chemicals. However, the timing of the peak apoptotic cell number was clearly delayed in the cases of busulfan and 6-mercaptopurine<sup>21</sup> than in the cases of other chemicals, although the cause of this difference is still unknown.

The detailed mechanisms of apoptotic cell death and cell cycle arrest induced in the fetal brain are considered to be different among DNA-damaging agents<sup>24–27</sup>. In addition, the exact mechanisms of busulfan-induced cytotoxicity in the fetal CNS remains unclear. The present results may provide not only fundamental information about systemic fetal tissue damage by busulfan but also a clue for elucidating the exact mechanisms of busulfan-induced cytotoxicity, especially in the fetal brain.

## Acknowledgements

The authors gratefully acknowledge Dr. Kunio Doi, Emeritus Professor of the University of Tokyo, for critical review of the manuscript.

## References

1. Bishop JB and Wassom JS. Toxicological review of busulfan (Myleran). *Mutat Res.* **168**: 15–45. 1986.
2. Nagai H. Effects of transplacentally injected alkylating agents upon development of embryos. Appearance of

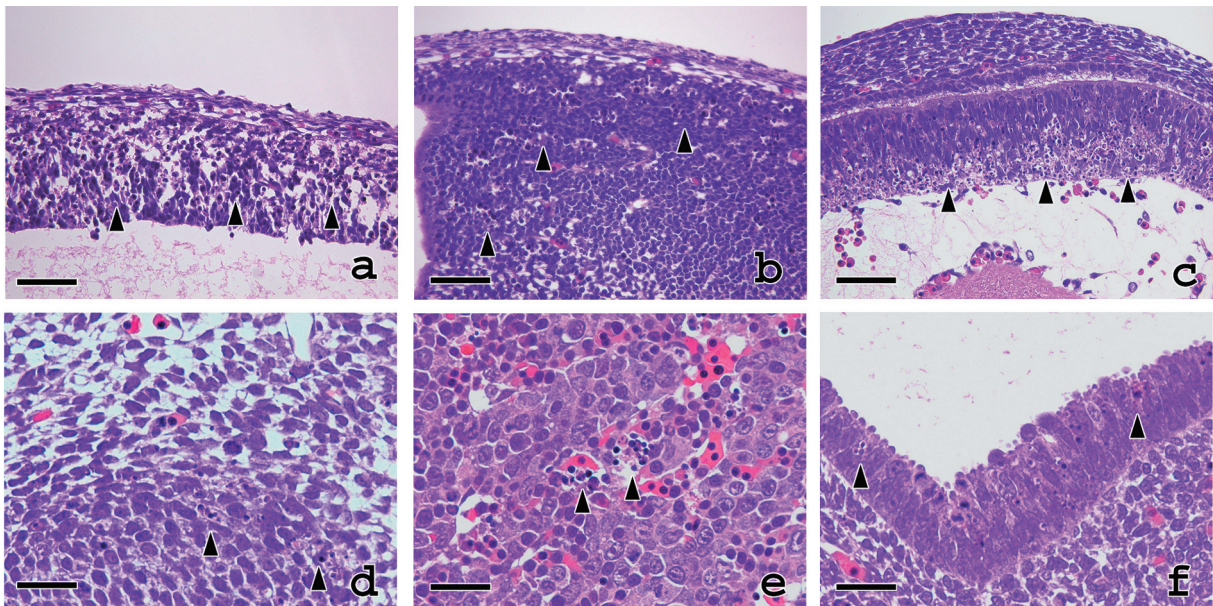


**Fig. 4.** Histopathology of the telencephalic wall (a), spinal cord (b), eye (c), mandible mesenchymal tissue (d), liver (e) and alimentary tract (f) in fetuses at 36 HAT. The number of pyknotic cells (arrowheads) is different among the tissues affected. HE stain. The bars are 50  $\mu\text{m}$  for a to c and 25  $\mu\text{m}$  for d to f.

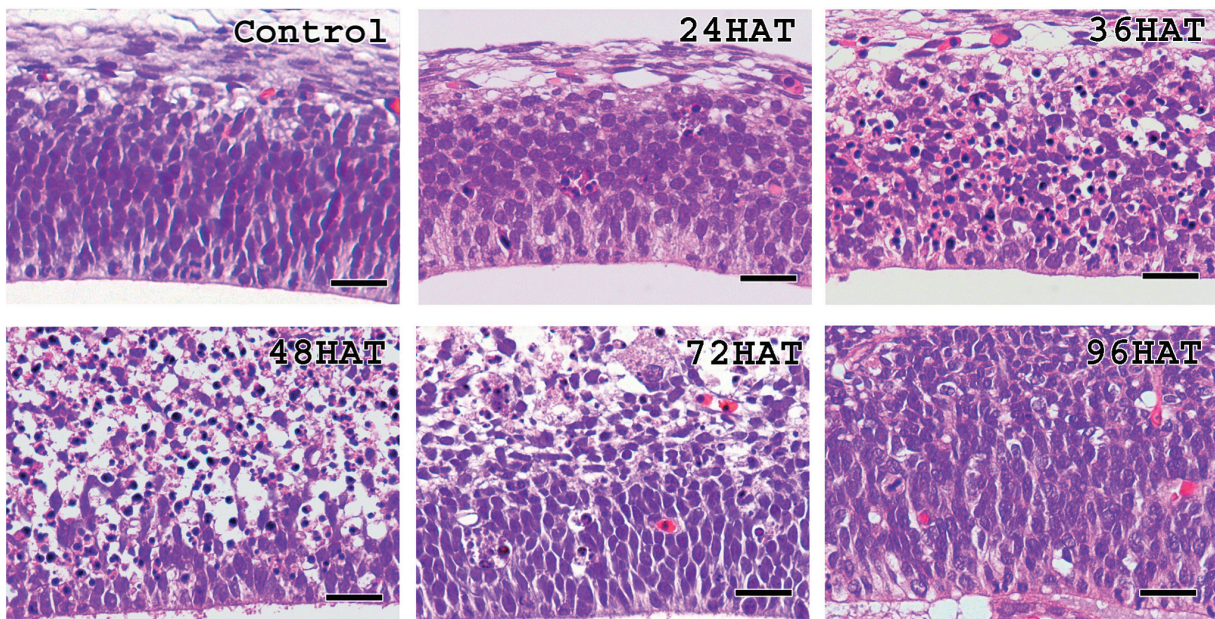


**Fig. 5.** Histopathological sequence of the telencephalon. The number of pyknotic neuroepithelial cells peaked at 36 or 48 HAT. As compared with the control at 48 HAT, the number of mitotic neuroepithelial cells in the ventricular layer decreased at 48 HAT. HE stain. Bar=25  $\mu\text{m}$ .

- intrauterine death and mesodermal malformation. *Bull Tokyo Dent Coll.* **13**: 103–119. 1972.
- Furukawa S, Usuda K, Abe M, and Ogawa I. Microencephaly and microphthalmia in rat fetuses by busulfan. *Histol Histopathol.* **22**: 389–397. 2007.
  - Kasuga F and Takahashi M. The endocrine function of rat gonads with reduced number of germ cells following busulphan treatment. *Endocrinol Jpn.* **33**: 105–115. 1986.
  - Otsuji M, Takahara M, Naruse T, Guan D, Harada M, Zhe P, Takagi M, and Ogino T. Developmental abnormalities in rat embryos leading to tibial ray deficiencies induced by busulfan. *Birth defects Res A Clin Mol Teratol.* **73**: 461–467. 2005.
  - Trams EG, Nadkarni MV, de Quattro V, Maengwyn-Davies GD, and Smith PK. Dimethane-sulphonoxybutane

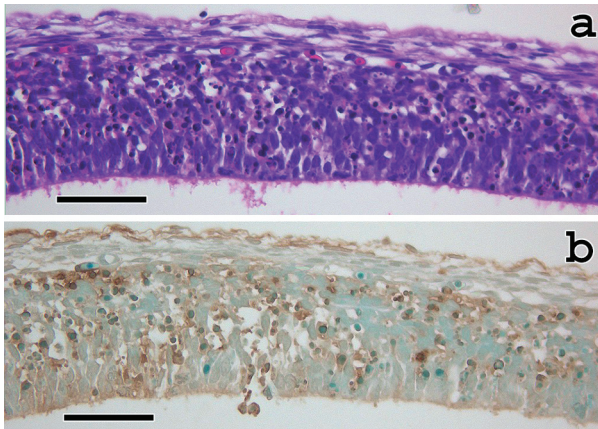


**Fig. 6.** Telencephalon of the busulfan group. The pyknotic cells on the HE-stained section (a) are positively stained by the TUNEL method (b). Bar=50  $\mu$ m.

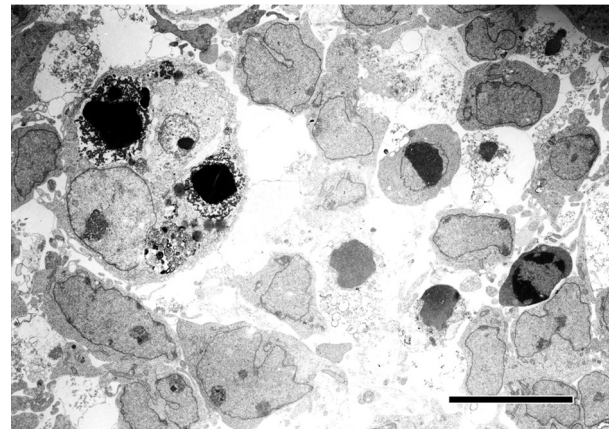


**Fig. 7.** Ultrastructure of pyknotic cells in the telencephalon at 48 HAT. Condensation of the nuclear chromatin of neuroepithelial cells and phagocytosis of apoptotic bodies by macrophages are shown. Bar=10  $\mu$ m.

- (Myleran) preliminary studies on distribution and metabolic fate in the rat. *Biochem Pharmacol.* **2**: 7–16. 1959.
7. Fox BW, Craig AW, and Jackson H. The comparative metabolism of Myleran 35/S in the rat, mouse and rabbit. *Biochem Pharmacol.* **5**: 27–29. 1960.
  8. Nadkarni MB, Trams EG, and Smith PK. Preliminary studies on the distribution and fate of TEM, TEPA and myleran in the human. *Cancer Res.* **19**: 713–718. 1959.
  9. Edwards K and Jones AR. Studies with alkylating esters, IV. The metabolism of propane-1, 3-dimethone-sulphonate and its relevance to the mode of action of Myleran. *Biochem Pharmacol.* **20**: 1781–1786. 1971.
  10. Gureli N, Denham SW, and Root SW. Cytologic dysplasia related to Busulfan (Myleran) therapy. *Obstet Gynecol.* **21**: 466–470. 1963.
  11. Burns WA, MacFarland W, and Matthews MJ. Busulfan-induced pulmonary disease: report of a case and review of the literature. *Am Rev Respir Dis.* **101**: 408–413. 1970.
  12. Asano M, Odell TT, McDonald TP, and Upton AC. Radiomimetic agents and X-rays in mice and AET protectiveness. *Arch Pathol.* **75**: 250–263. 1963.
  13. Tange T. Significance of the bone marrow lymphocyte hematopoietic regeneration following acute injury due to cobalt-60 irradiation and cytotoxic drugs. *Acta Pathol Jpn.* **24**: 93–117. 1974.
  14. Katayama K, Ishigami M, Uetsuka K, Nakayama H, and Doi K. Ethylnitrosourea (ENU)-induced apoptosis in the rat fetal tissues. *Histol Histopathol.* **15**: 707–711. 2000.
  15. Yamauchi H, Katayama K, Yasoshima A, Uetsuka K, Nakayama H, and Doi K. 1- $\beta$ -D-arabinofuranosylcytosine (Ara-C)-induced apoptosis in the fetal tissues and placenta. *J Toxicol Pathol.* **16**: 223–229. 2003.
  16. Ueno M, Katayama K, Nakayama H, and Doi K. Mechanisms of 5-azacytidine (5Az-C)-induced toxicity in the rat foetal brain. *Int J Exp Path.* **83**: 139–150. 2002.
  17. Nam C, Woo GH, Uetsuka K, Nakayama H, and Doi K. Histopathological changes in the brain of mouse fetuses by etoposide-administration. *Histol Histopathol.* **21**: 257–263. 2006.
  18. Yamaguchi Y, Aoki A, Fukunaga Y, Matsushima K, Ebata T, Ikeya M, and Tamura K. 5-Fluorouracil-induced histopathological changes in the central nervous system of rat fetuses. *Histol Histopathol.* **24**: 133–139. 2009.
  19. Woo GH, Bak EJ, Nakayama H, and Doi K. Molecular mechanisms of hydroxyurea (HU)-induced apoptosis in the mouse fetal brain. *Neurotox Teratol.* **28**: 125–134. 2006.
  20. Gavrieli Y, Sherman Y, and Ben-Sasson SA. Identification of programmed cell death in situ via specific labeling of nuclear DNA fragmentation. *J Cell Biol.* **119**: 493–501. 1992.
  21. Kanemitsu H, Yamauchi H, Komatsu M, Yamamoto S, Okazaki S, and Nakayama H. Time-course changes in the neural cell apoptosis in the rat fetal brain from dams treated with 6-mercaptopurine(6-MP). *Histol Histopathol.* **22**: 317–324. 2009.
  22. Lu DP, Nakayama H, Shinozuka J, Uetsuka K, Taki R, and Doi K. 5-azacytidine-induced apoptosis in the central nervous system of developing rat fetuses. *J Toxicol Pathol.* **11**: 133–136. 1998.
  23. Furukawa S, Abe M, Usuda K, and Ogawa I. Indole-3-acetic acid induces microencephaly in rat fetuses. *Toxicol Pathol.* **32**: 659–667. 2004.
  24. Yamauchi H, Katayama K, Ueno M, Uetsuka K, Nakayama H, and Doi K. Involvement of p53 in 1- $\beta$ -D-arabinofuranosylcytosine-induced rat fetal brain lesions. *Neurotox Teratol.* **26**: 579–586. 2004.
  25. Ueno M, Katayama K, Yamauchi H, Nakayama H, and Doi K. Cell cycle and cell death regulation of neural progenitor cells in the 5-azacytidine (5AzC)-treated developing fetal brain. *Exp Neurol.* **198**: 154–166. 2006.
  26. Katayama K, Ueno M, Yamauchi H, Nakayama H, and Doi K. Ethylnitrosourea induces neuronal progenitor cell apoptosis after S-phase accumulation in a p53-dependent manner. *Neurobiol Dis.* **18**: 218–225. 2005.
  27. Nam C, Yamauchi H, Nakayama H, and Doi K. Etoposide induces apoptosis and cell cycle arrest of neuroepithelial cells in a p53-related manner. *Neurotox Teratol.* **28**: 664–672. 2006.